2023 IEEE/ACM International Workshop on Search-Based and Fuzz Testing (SBFT) | 979-8-3503-0182-3/23/$31.00 ©2023 IEEE | DOI: 10.1109/SBFT59156.2023.00012

On the Strengths of Pure Evolutionary Algorithms in Generating Adversarial Examples

Antony Bartlett
Delft University of Technology
Delft, the Netherlands
a.j.bartlett@tudelft.nl

Cynthia C. S. Liem
Delft University of Technology
Delft, the Netherlands
c.c.s.liem@tudelft.nl

Annibale Panichella
Delft University of Technology
Delft, the Netherlands
a.panichella@tudelft.nl

***Abstract*—Deep learning (DL) models are known to be highly accurate, yet vulnerable to adversarial examples. While earlier research focused on generating adversarial examples using white-box strategies, later research focused on black-box strategies, as models often are not accessible to external attackers. Prior studies showed that black-box approaches based on approximate gradient descent algorithms combined with meta-heuristic search (i.e., the `BMI-FGSM` algorithm) outperform previously proposed white- and black-box strategies. In this paper, we propose a novel black-box approach purely based on differential evolution (DE), i.e., without using any gradient approximation method. In particular, we propose two variants of a customized DE with customized variation operators: (1) a single-objective (`Pixel-SOO`) variant generating attacks that fool DL models, and (2) a multi-objective variant (`Pixel-MOO`) that also minimizes the number of changes in generated attacks. Our preliminary study on five canonical image classification models shows that `Pixel-SOO` and `Pixel-MOO` are more effective than the state-of-the-art `BMI-FGSM` in generating adversarial attacks. Furthermore, `Pixel-SOO` is faster than `Pixel-MOO`, while the latter produces subtler attacks than its single-objective variant.**

***Index Terms*—differential evolution, adversarial examples, deep learning, search-based software engineering**

I. Introduction

Many systems we encounter in daily life include machine learning components that make automated decisions or inferences based on observed data patterns. Ever since so-called deep convolutional neural networks outperformed hand-crafted methods in the 2012 ImageNet Large-Scale Visual Recognition Challenge (ILSVRC) [26], deep learning models have become mainstream in computer vision, but also in many other applied machine learning domains, such as natural language processing and music information retrieval.

Deep learning models have been lauded for yielding high-accuracy predictions and, thus, have become attractive candidates for integration in real-life systems that may be safety-critical (e.g. vision components in self-driving cars). At the same time, they have been criticized for making intolerable and sometimes incomprehensible prediction errors, jeopardizing safety. As has been shown in the machine learning world, they are e.g. inherently vulnerable to so-called adversarial attacks, in which perceptually small changes to input data can cause very different, erroneous model predictions [11], [34].

Adversarial examples have been extensively investigated in the literature, where the idea is to introduce subtle changes in the data (e.g., changing the pixels in a target image) that do not change the ground truth but make a DL model predict incorrect output. Existing approaches to adversarial example generation can be classified into white-box and black-box methods. White-box approaches [12], [16], [20], [25], [35], [37] require access to the model under test (i.e. the model architecture, neuron weight values, and gradients). Black-box strategies [19], [23], [31], [32], [39], instead, only require access to model inputs and outputs. These approaches are considered more realistic as it reflects what external attackers can obtain [19], e.g., in the case of remote API access.

Therefore, in this paper, we focus on black-box strategies and target deep neural network (DNN) models for image recognition. In this field, the state-of-the-art approach by Lin et al. [19] uses the *Black-box Momentum Iterative Fast Gradient Sign Method* (`BMI-FGSM`) to approximate the gradient based on a few data points. These points are obtained by mutating existing images (seeds) with *evolutionary algorithm* (EA), and *differential evolution* (DE) in particular. Their results showed that `BMI-FGSM` outperforms white-box and black-box approaches previously proposed in the literature.

Despite these undisputed results, we observe that `BMI-FGSM` requires thousands of iterations to successfully generate adversarial attacks, despite the usage of gradient-based methods. In this paper, we investigate the usage of DE alone —i.e., without employing gradient-based methods— as the core technique to generate adversarial attacks in a black-box fashion. In particular, we introduce three customized operators for DE that introduce perturbations (pixel changes) in the target images. We focus on DE as meta-heuristics since they can outperform gradient-based approaches (e.g., reinforcement learning) as reported in recent studies [27].

We introduce two variants of DE: (1) a single-objective variant (`Pixel-SOO`) that steers for pixel-based input changes to cause an output prediction to change gradually; (2) a multi-objective variant (`Pixel-MOO`) that additionally seeks to minimize the number of pixel modifications made to the original input image. Then, we conduct a preliminary study focused on answering the following research questions:

RQ1 : *How do `Pixel-SOO` and `Pixel-MOO` perform compared to the state-of-the-art `BMI-FGSM` in generating adversarial attacks?*

RQ2 : *What are the strengths and weaknesses of `Pixel-SOO` and `Pixel-MOO`?*

The results of our study with five DNN models show that the proposed DE-based approaches are more effective in generating adversarial attacks than `BMI-FGSM` despite not using any gradient-based methods. In particular, `BMI-FGSM` struggles to generate adversarial examples for all DNNs under test; besides, when successful, it required more generations than `Pixel-MOO` and `Pixel-SOO`. Instead, our approaches are always able to generate attacks within the same search budget used for `BMI-FGSM`. Finally, we discover that `Pixel-MOO` and `Pixel-SOO` provides two different trade-offs. The former generates attacks with fewer and more subtle changes than the latter, but requires more generations to converge.

II. Related Work

As discussed in our Introduction, white-box testing [12], [16], [20], [25], [35], [37] has been extensively researched, but needs internal model access, which is not always realistic in practice. Therefore, we will adopt a black-box testing approach instead, which purely focuses on modifying a system's input (in our case, an image) to trigger undesired changes in the system's output (in our case, the object classification for the input image). We will employ evolutionary strategies for this; beyond images, these have e.g. been proposed on credit scoring models [10] and speech audio [14], [15].

In literature, various black-box attacks on image recognition DNNs have been proposed [19], [23], [39]. Nguyen et al. [23] generate random images that are noise to humans, but are misclassified as actual objects by a DNN. In our case, we will seek more adversarial examples, where input is kept as close to the original as possible (and thus human-recognizable).

Zhou et al. [39] propose a hybrid black-box approach that combines EAs with the bisection method. The images are mutated by injecting full black or white pixels. Instead, Chan and Cheng [4] introduced a black-box approach that adds Gaussian noise to large portions of the images. Besides, their work targets object detection models rather than image recognition. In contrast, our paper investigates the adversarial example generation in a multi-objective variant where both (1) the model misclassification and (2) the number of changed pixels are taken into account.

Several works explicitly focused on minimizing perturbations, such that fewer modifications to an image would already lead to different system output. One example of this is the work by Suzuki et al. [32], which proposes a Discrete Cosine Transform-based method for modifying images. While such perturbations parametrically are small, they still will affect many pixels at once. A similar consideration holds for the work by Sun et al. [31], focusing on minimum visibility of the modification from a perceptual perspective, but not explicitly constraining the number of pixels to modify.

On the other end of the extreme, one may search for attacks that modify as few pixels as possible (and as such will naturally not stand out, when compared to the total amount of pixels in an image). For example, Su et al. [30] propose a single-pixel adversarial attack using DE, executed against the classical CIFAR-10[1] [17] and ImageNet object classification datasets. Comparing the results on these two datasets, a high success rate is reported for CIFAR-10, but this success rate is much lower for ImageNet, where single-pixel attacks mainly succeed in situations where the original classification of the image was already quite low. This may have to do with the difference in search space; the test images in CIFAR-10 are much smaller ($32 \times 32 = 1024$ pixels) than those in ImageNet ($224 \times 224 = 50,176$ pixels).

A stronger, yet compact attack is proposed by Lin et al. [19], who combined DE [29] and the Fast Gradient Sign Method [22] for black-box adversarial sample generation. Executing a single-objective attack called `Black-box Momentum Iterative Fast Gradient Sign Method (BMI-FGSM)`, to generate an efficient and effective perturbation that is similar to the benign input. Their approach utilizes double-step size and candidate reuse whilst approximating the gradient direction. An initial gradient sign population is generated using DE. The input is then gradually modified using gradient sign approximation until an adversarial example is created that is visibly the same as the original input, but now classified as something different. Lin et al. [19] showed that `BMI-FGSM` successfully generates adversarial examples for large models, outperforming other state-of-the-art white-box and black-box approaches.

While Lin et al. [19] showed that black-box approaches based on EAs can be very competitive with their white-box alternatives, existing approaches have various drawbacks. First, `BMI-FGSM` requires a large number of iterations (in the order of thousands) and population size (hundreds of individuals). In other words, attackers need to query the model under attack many times, increasing the chances of detection. Second, `BMI-FGSM` combines multiple techniques, making its implementation less trivial and introducing more hyper-parameters to tune. Finally, the generated attacks are not minimal, i.e., the prediction flip is achievable but requires changing all pixels in the original image (or seed).

In this paper, we introduce a simpler approach purely based on DE. Furthermore, we introduce both a single- and multi-objective variant of our approach. The former focuses on flipping the model prediction, while the latter considers an additional objective that aims to directly minimize the number of modified pixels. As our results will show, our approach requires a much lower number of model queries and introduces fewer image changes compared to `BMI-FGSM`.

III. Approach

Without loss of generality, an image classifier f is a mathematical function/model $f : I \longrightarrow L \times \mathbb{R}^n$, which takes as input an image $i \in I$ and returns a label $l \in L$ and a confidence vector $conf \in \mathbb{R}^n$, which contains the probabilities associated with all labels $l \in L$ in descending order. The first element $conf_1$ is the probability associated with

[1]https://www.tensorflow.org/datasets/catalog/cifar10

the most likely (predicted) label l, while the remaining entries in $conf_2 \ldots conf_n$ are related to the other possible labels $\in L$. We can now reformulate adversarial attack generation as a search problem:

Definition 1: Let $f : I \longrightarrow L \times \mathbb{R}$ be a trained model that takes as input an image $i \in I$ and returns a predicted label $l \in L$. Let $m : I \longrightarrow I$ be a transformation function that mutates (i.e. applies changes to) an image $i \in I$. The problem is finding a mutated image $m(i)$ such that $f(m(i)) \neq f(i)$, with the constraints that both i and $m(i)$ share the same correct label (same ground truth).

Attack generation strategies can be *targeted* or *un-targeted*. The former aims to flip the prediction to a specific label or classification outcome, while the latter aims to lead the model toward producing any incorrect outcome. In this paper, we focus on un-targeted attack generation: for demonstrating the vulnerability of a machine learning model, it is sufficient to generate mutated images $m(i)$ that flip the predicted output to any other label than the ground truth label. Since a classification model returns both the label and the corresponding confidence level, we can use the latter to guide the search toward the flipped prediction. More precisely, given a classification model $f : I \longrightarrow L \times \mathbb{R}$, a seed image i, and its mutated variant $m(i)$, we optimize the following objective:

$$\min O_1 = \begin{cases} f(m(i))_1^{conf} - f(m(i))_2^{conf} & \text{if } f(i)_1^l = f(m(i))_1^l \\ -f(m(i))_1^{conf} & \text{if } f(i)_1^l \neq f(m(i))_1^l \end{cases} \tag{1}$$

In other words, this objective aims to reduce the confidence for the most likely prediction/label ($f(m(i))_1^{conf}$), while increasing the confidence for the second-most-likely prediction ($f(m(i))_2^{conf}$). Therefore, the overall goal is to reduce the difference between the top-2 labels until the model f flips the prediction to a different label (condition $f(m(i))_1^{label} \neq f(m(i))_1^{label}$). In general, Equation 1 takes values in [-1,1]. A zero value indicates that the models assign equal confidence scores to the top-2 labels. A negative value indicates that the model f flips the prediction to a different label, whose confidence level corresponds to the absolute value of Equation 1.

We can expand this to a multi-objective problem where both "fooling" the model and reducing the number of perturbations (at the pixel level) are equally important:

Definition 2: The problem is finding a mutated image $m(i)$ such that $f(m(i)) \neq f(i)$ and that minimizes the distance $d(i, m(i))$, with the constraints that both i and $m(i)$ share the same correct label (same ground truth).

Beyond flipping the prediction outcome by optimizing for O_1, we now also need an additional objective to guide the search towards minimizing the difference between the original image i and its mutated counterpart $m(i)$. To this end, our second objective counts the number of pixels that differ between the seed image i and the mutated image $m(i)$:

$$\min \ O_2 = \pi(m(i[a,b]) \neq i[a,b]) \tag{2}$$
$$= |\{e_a, b \in i : i[a,b] \neq m\left(i[a,b]\right)\}| \tag{3}$$

where $i[a,b]$ and $m\left(i[a,b]\right)$ denote the pixel values in row a and column b for the two images i and $m(i)$, respectively.

These two objectives are *conflicting*. A simple solution for O_1 may consist of changing all pixels in the original figure i such that the object is no longer recognizable for the model f. However, such a solution would not be optimal for O_2. Vice versa, a new image with zero alteration would be optimal for O_2, but not flip the prediction as sought by O_1.

Given the conflicting nature of our objectives, it is not possible to find one single solution that simultaneously optimizes them all. In other words, the problem is inherently multi-objective where the goal becomes to find the set of optimal trade-offs between O_1 and O_2. In particular, we aim to find *Pareto efficient* trade-offs based on the concepts of *dominance* and *Pareto optimality*.

A. Single and Multi-objective Differential Evolution

To find adversarial attacks, we rely on differential evolution (DE) only. Hence, compared to `BMI-FGSM`, we do not use any algorithm to approximate the gradient. We consider two different variants of DE: `Pixel-SOO`, a traditional single-objective variant (to optimize O_1) and `Pixel-MOO`, a multi-objective variant based on the *non-dominated sorting algorithm* (NSDE) [2] (to optimize O_1 and O_2).

Both variants iteratively evolve a pool of N randomly generated adversarial attacks, called *population*. In each iteration, N offspring attacks are generated from the population using variation operators. Then, the population for the next iteration is obtained by combining the previous population and the offspring attack, forming a pool Q of $2 \times N$ attacks and selecting the N top individuals. The selection is performed using an *environmental selection* and represents the main difference between `Pixel-SOO` and `Pixel-MOO`. In `Pixel-SOO`, the *environmental selection* is applied by selecting the best N individuals among the parent and the offspring solutions/attacks according to the main objective O_1. This mechanism is *elitist* since the best attacks can survive across the generations until new better solutions are found. In `Pixel-MOO`, the *environmental selection* is performed by applying the *fast non-dominated sorting algorithm* [8], which ranks the solutions in Q into sub-dominated fronts based on the dominance relation.

In the following, we detail (1) the encoding schema, (2) how we initialize the initial population, (3) the variation operator.

1) Encoding schema: As mentioned before, an adversarial attack is produced by altering a seed image i. Instead of representing/encoding an adversarial attack as a completely new image, we only encode the changes to be applied, also called the *mask*. In particular, given the seed image i, we encode a solution/attack in NSDE as a list of pixels to change: $X = [x_1, \ldots, x_k]$. Each entry x_j in X is a tuple $[a, b, value_j]$, where a and b determine the position of the pixel to change (i.e., a is the row index and b is the column index), while $value_j$ indicates the new pixel value in RGB notation.

2) Initialization: The first step to initializing NSDE involves generating an initial pool of adversarial attacks. To this aim, we create N attacks by creating an empty mask $X = []$ and adding some changes using the *add* operator, one of three alternative variation operators described below.

3) Variation operator: Given a parent attack X, we design three types of operators that *add*, *delete*, or *change* entries in X. Each operator is applied with probability 1/3.

The **add** operator randomly inserts one entry in X with probability $\sigma = 1$; a second entry is added with probability $\sigma = 0.5$; the third one with probability $\sigma = 0.25$; and so on until no other element is added. To add a new element/entry x in X, this operator randomly selects one pixel from the original seed image i with position row_j and col_j and draws three random (noise) values $\delta(\mu, \lambda)$ from a Gaussian distribution with mean μ and standard deviation λ, that will be applied to the respective R, G and B channels. Hence, the new entry x will be equal to $[row_j, col_j, value_j + \delta(\mu, \lambda)]$.

The **delete** operator simply deletes one entry/tuple from the mask X. However, this operator is applied only if X contains at least two entries. This operator plays a critical role in our multi-objective formulation as it allows to remove spurious pixel changes that do not contribute to changing the prediction results of the model f under test.

The **change** operator changes the pixel values using the traditional *differential operator*. Given a parent image to mutate X and a donor solution Y, a new solution X' is formed by using the following formula:

$$X'[a,b] = \begin{cases} R_1[a,b] + F \cdot (R_2[a,b] - Y[a,b]) & \text{if } r < CR \\ X[a,b] & \textit{otherwise} \end{cases} \tag{4}$$

where $r \in [0, 1]$ is a randomly generated number; R_1 and R_2 are other solutions within the population. There are various variants of the differential operator that differ in how X_1, X_2, and the donor solution Y are selected. In this paper, we use the standard `DE/rand/1` variant, where `rand` indicates that the donor Y is randomly selected, while `1` indicates there is only one donor solution. Finally, the other solutions R_1 and R_2 are always randomly selected from the population.

In Equation 4, $F \in [0, 2]$ is called *scaling factor* and establishes how far the new solution X' is from the original solution X based on the differentials values of the donor solution Y. Hence, F balances both exploration and exploitation. Finally, $CR \in [0, 1]$ is the *crossover rate* and determines how many pixels in X will be changed.

We apply a small tweak in our context compared to the traditional differential operator. If the pixel $X[a, b]$ differs from the original seed solution, Equation 4 may remove this change if $R_1[a, b]$, $R_2[a, b]$, and $Y[a, b]$ are identical to the original seed image. To prevent this case, we set the pixel $R_1[a, b] = [0, 0, 0]$ (in RGB notation) if $R_1[a, b]$ is identical to the pixel of the initial image/seed. The same is done for $R_2[a, b]$ and $Y[a, b]$. Notice that this tweak is applied only if $X[a, b]$ differs from the original seed's pixel in row a and column b.

B. Additional Remarks

`BMI-FGSM` by Lin et al. [19] and our approach share the main goal of flipping the label prediction. However, there are critical differences that are worth highlighting. The first difference regards the main objective or fitness function. The main (single) fitness function used by `BMI-FGSM` aims to "*suppress the probability of the ground-truth label*" [19] until another false label is predicted. Our O_1 explicitly maximizes the confidence level for the false label, even after the prediction has been flipped (second case in Equation 1).

The most critical difference is within the variation operator. `BMI-FGSM` combines differential operators and the *iterative fast gradient sign method*. Instead, `Pixel-MOO` and `Pixel-SOO` rely on the differential operators but introduce two novel ways to generate offspring: (1) the *add* and (2) *delete* operators introduced in Section III-A. The latter allows deleting pixel changes that do not contribute to optimizing O_1 (for `Pixel-SOO`) or that are not Pareto efficient w.r.t. O_1 and O_2. (for `Pixel-MOO`). Finally, `Pixel-MOO` explores multi-objective optimization where the mask size is considered as an explicit objective with the goal of generating minimal adversarial attacks. Instead, `BMI-FGSM` targets only the prediction outcome and does not constrain the number of pixels that can be altered to reach a prediction flip.

IV. Empirical Evaluation

To answer our RQs, we run our approach with 5 different, well-known deep computer vision models from the `Keras` python library. We chose `VGG16` and `VGG19` which are both classified as "very deep" convolutional neural networks for large-scale image recognition[2] [28], that got a canonical status due to their strong performance in the `ImageNet` benchmark challenges[3]. VGG16 was one of the best-performing models in the 2014 ILSVRC challenge and achieves 92.7% top-5 test accuracy on the ImageNet dataset. VGG16 and VGG19 both consist of 3x3 convolutional layers stacked on top of each other in increasing depth, with VGG16 having 16 convolutional layers, and VGG19 being 'deeper' with 19 convolutional layers. Furthermore, `ResNet50`, `ResNet101` and `ResNet152` all are based on deep residual learning for image recognition[4] [13]. In our experiments, we use the ImageNet pre-trained weights released by the original authors after training on the ILSVRC2012 training set, as released through Keras [5]. Note that despite these details, we consider all models as a black-box, given the fact that our approach (and the baseline) does not need access to the model internals.

A. Dataset

For our experiments, we sample 50 images from the ImageNet ILSVRC2012 Validation data set [26]. We chose the validation set, due to a lack of ground-truth data availability for the test set. First, we draw an initial pool of images for

[2]https://keras.io/api/applications/vgg/
[3]https://image-net.org/challenges/LSVRC/index.php
[4]https://keras.io/api/applications/resnet

the input by selecting 1000 random images from the ImageNet validation data folder. After pre-processing the images to have a 224×224 input size, we then choose whether to drop or retain the image based on the prediction confidence by the VGG19 model and class uniqueness. As for the prediction confidence, if the correct ground truth label is predicted with confidence between 0.8 and 0.9, we consider the image to be a valid image for our experiments: as the ground truth label is recognized with high confidence, we can be confident it is visually distinguishable and not ambiguous w.r.t. other classes; at the same time, for too high confidence, it may be too obviously one particular image class, and flipping may as a consequence be hard. By retaining only one image per object class, we also ensure a reasonably diverse set of images.

B. Implementation and Parameter settings

We have implemented the different DE-based approaches in `Pymoo` v0.5.0 [3], using Python 3.10 and `Keras` 2.2.2. Pymoo [3] is an open-source framework that allows us to easily adapt the simple DE and the NSDE for generating adversarial attacks. Runs are evaluated inside a Docker container on an AMD EPYC 7713 64-Core Processor running at 2.6 Ghz and with 256 available CPUs. We had 3 Nvidia A40 GPUs each with 48 GB GDDR6 running CUDA version 11.6 available to us. The Dockerfile in our implementation can be rebuilt on any system, easily modifying the CUDA container for a different system. Our implementation is available on Zenodo: *https://doi.org/10.5281/zenodo.7741267*

Due to issues with running the code from `BMI-FGSM`, we were not able to execute it using CUDA [1] (GPU). This meant we could only run the baseline on CPU, which has likely resulted in a slower execution time compared to our multi-objective results which were executed on GPU.

Parameters setting. We set both the multi-, single-objective DE, and `BMI-FGSM` to evolve a population size of 20 over a maximum of 400 generations. When a test image has been wrongly predicted, we kill the test and allow it to run for five more generations, so better fronts may still be found. For the parameter settings, we have chosen the same values as suggested in the literature [8], [21].

We use the variation operators as described in Section III with a crossover rate $CR = 0.9$ and scaling factor $F = 0.8$, which are the recommended values in the literature [21]. For both algorithms, solutions/attacks are selected for reproduction using the binary-tournament selection [8]. For `Pixel-SOO`, the binary selection is based on the single-objective value to optimize (i.e., O_1). Instead, in `Pixel-MOO`, the selection relies on dominance to decide which solution wins each tournament round. Finally, we opted for a relatively small population size $p = 20$ (smaller than p=100 used in other studies [19], [21]) as suggested in the literature from problems with expensive objective computation [6].

C. Study Design

To answer our first research question, we compare our multi-objective approach `Pixel-MOO` to our single-objective approach `Pixel-SOO` (only optimizing for O_1); next to this, we compare our single-objective approach to the `BMI-FGSM` method by Lin et al. [19]. In this, we try to stay as close to the implementation by the authors as possible; as a consequence, beyond the parameters setting population size and generations, we do not modify the authors' codebase[5]. The `BMI-FGSM` codebase only supports VGG16, ResNet50 and ResNet101; here, we started our experiments with VGG16. We execute `BMI-FGSM`, `Pixel-SOO` and `Pixel-MOO` against each image in our dataset to generate adversarial examples. For each image, we run each algorithm 10 times, to account for their random nature. As a consequence, with 50 images, the end result is a total of 1500 test runs (500 for each method). For each of the `Pixel-SOO` and `Pixel-MOO` executions, a new random seed was generated and stored for future replications, together with the results of the generated attacks. For `BMI-FGSM` a slight modification was made to the codebase to output the current prediction data. This data is stored for each run, along with the adversarial image.

For evaluation, we consider two performance metrics: (1) the success rate, indicating the percentage out of the 10 runs for which `Pixel-SOO` and `Pixel-MOO` were capable of causing a change in prediction output, and (2) how many pixels needed modification (i.e., how many tuples are in mask X) in the best solution. For the comparison, we considered the best solution/attack in the final population (last generation) of `Pixel-SOO`. Instead, `Pixel-MOO` provides a set of non-dominated solutions (front) rather than one single solution. For our analysis, among all solutions/attacks that lead to flipping the prediction (i.e., those with negative values for the first objective O_1), we have chosen the one with the lowest number of changed pixels (second objective O_2).

To compare `BMI-FGSM` and `Pixel-MOO`, we analyze the success rate in flipping the prediction and the median number of changes required to flip the model's prediction over the 10 runs. We also apply statistical analysis to further assess whether the observed differences are significant or not. We use Fisher's exact test [9] for the success rate, considering the results of each run (for each algorithm) as a binary/dichotomy outcome (i.e., the prediction was flipped or not). To assess the significance of the differences among `Pixel-SOO` and `Pixel-MOO` w.r.t. the number of altered pixels, we use the Wilcoxon rank sum test [7]. For both statistical tests, we use a confidence level $\alpha = 0.95$. Furthermore, we complement the test for significance with the Vargha-Delaney statistic ($\hat{A}_{12}$) to measure the effect size of the results [36].

D. Results

Results on VGG16. A full breakdown of the VGG16 results can be seen in Figure 1, which depicts the success rate of `BMI-FGSM`, `Pixel-SOO` and `Pixel-MOO` in creating adversarial examples for the 50 images in our experiment. As we can observe, `BMI-FGSM` was rarely able to flip the predictions for VGG16 (median, second, and third quartiles

[5]https://github.com/jylink/BMI-FGSM

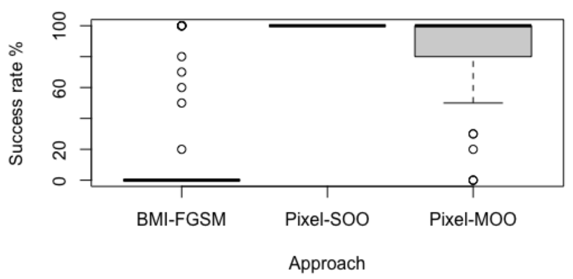

Fig. 1: Success rate of `BMI-FGSM`, `Pixel-SOO` and `Pixel-MOO` in flipping the predictions for VGG16.

Seed	**Perturbations**			**# Generations**			**Runtime (seconds)**		
Image	BMI	P-Soo	P-Moo	BMI	P-Soo	P-Moo	BMI	P-Soo	P-Moo
00323	4325	25	14	240	10	18	2850	73	98
00344	-	16	13	-	6	12	-	57	77
00624	-	55	51	-	21	42	-	126	237
01204	-	39	29	-	13	22	-	87	124
02431	10620	19	18	20	10	24	227	74	123
05053	-	155	129	-	65	180	-	336	847
05412	-	65	36	-	34	128	-	188	631
05929	-	76	83	-	30	71	-	168	371
06213	-	159	92	-	76	184	-	393	1897
07160	-	70	76	-	27	70	-	153	336
08024	-	35	39	-	19	44	-	117	247
09335	-	17	11	-	9	11	-	69	72
09485	-	137	96	-	70	297	-	363	1749
09654	-	65	46	-	31	111	-	175	532
09931	-	36	22	-	11	22	-	83	104
11100	-	24	11	-	9	17	-	73	88
11177	-	69	55	-	26	68	-	150	326
11189	-	30	19	-	9	15	-	72	88
12820	-	114	100	-	43	95	-	234	473
14504	-	79	72	-	33	139	-	184	710
15116	7391	30	31	240	17	55	2852	105	292
15739	-	57	33	-	25	62	-	144	324
16615	-	39	32	-	12	24	-	83	116
20018	NA	43	39	NA	25	82	NA	147	398
20889	-	112	102	-	65	237	-	335	1138
23090	-	162	134	-	70	217	-	360	1053
23203	10246	151	140	320	64	286	3763	334	1381
23729	-	82	56	-	39	123	-	214	609
24130	-	41	24	-	27	77	-	151	406
25633	-	127	121	-	47	97	-	248	472
26738	-	67	61	-	22	41	-	132	219
27242	4885	12	6	320	4	8	3797	48	48
29251	6593	26	17	320	12	23	3790	84	124
30019	-	64	51	-	23	57	-	136	285
30959	4774	38	32	120	17	30	1449	106	160
32263	12507	23	15	80	7	12	966	61	67
32576	-	81	72	-	38	101	-	205	513
34966	-	45	39	-	17	34	-	109	182
35091	-	34	24	-	11	21	-	80	105
35614	-	83	59	-	45	155	-	235	956
36183	15992	26	22	0	10	16	44	76	104
38221	-	37	20	-	60	93	-	307	1891
41173	-	101	91	-	94	241	-	463	1523
41842	-	173	129	-	81	377	-	408	1903
43541	-	46	36	-	19	32	-	120	180
44582	-	113	119	-	51	201	-	267	1005
44788	-	80	24	-	61	61	-	313	1919
46372	11463	35	28	40	14	30	505	95	156
46979	-	49	39	-	18	31	-	111	158
48219	4244	24	16	320	8	12	1180	66	71
Mean	8872	67	54	178	32	90	1857	176	547

TABLE I: Median number of pixel changes, generations, and running time required by all approaches to generate adversarial attacks on VGG16.

being equal to zero), while our approaches based on pure DE can do so for all images. By comparing `Pixel-SOO` and `Pixel-MOO`, we observe that the former always achieves a 100% success rate while the latter achieves a lower success rate in 20% of the images. However, both our DE-based approaches can generate an adversarial attack in at least one of the ten repetitions.

To better understand the time needed to converge and how many pixels have been changed by the different algorithms, we report in Table I the detailed results for each image in our benchmark. In particular, we report the running time, the number of changes (altered pixels), and the generations required for flipping our image prediction. In Table I, "–" entries indicate that the corresponding algorithm could not generate an adversarial attack within the search budget. We can observe that `BMI-FGSM` successfully generated adversarial attacks (at least in one out of 10 runs) for 11 images out of 50. To do so, it changed thousands of pixels (8872 on average) and up to 15992 pixels for the image 'ILSVRC2012_val_00036183.JPEG' (in short, image id = 36183 in Table I). The image 'ILSVRC2012_val_00020018.JPEG' is an interesting case since `BMI-FGSM` threw an error when loading the image (highlighted with NA values in Table I).

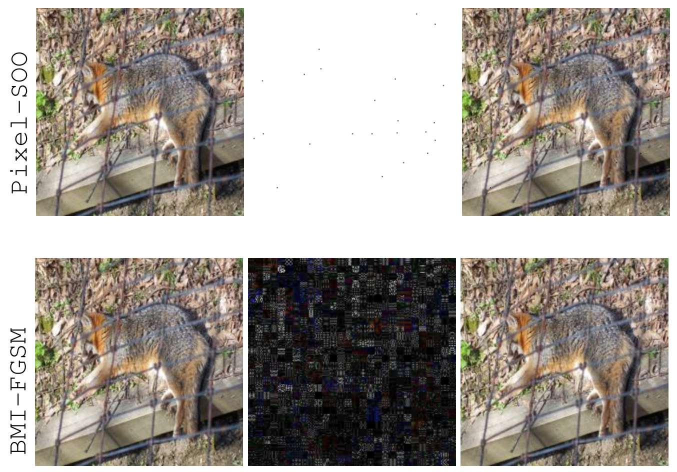

(a) Original image (b) Mask (c) Final image

Fig. 2: `Pixel-SOO` vs. `BMI-FGSM` results for Image 'ILSVRC2012_val_00000323.JPEG'

Instead, both `Pixel-SOO` and `Pixel-MOO` were able to generate adversarial attacks for all the images in at least 1 of the ten individual runs. Indeed, there is no "-" entry in Table I for these two algorithms. W.r.t. the number of introduced changes, we can observe that both algorithms required to change fewer pixels than the state-of-the-art `BMI-FGSM`. `Pixel-SOO` changed on average 67 pixels while `Pixel-MOO` generated successful attacks by changing even fewer pixels (54 pixels on average).

To better understand the type of attacks generated by `Pixel-MOO` and the baselines `BMI-FGSM`, Fig. 2 shows the results of the first image in our dataset 'ILSVRC2012_val_00000323.JPEG'. This is one of the few images for which `BMI-FGSM` could successfully generate an adversarial attack. The original image was ground-truthed and classified as a 'grey fox' (67). When initially running the image through `BMI-FGSM`, the classification was shown as 'garbage truck, dustcart' (280). This is an incorrect classification and may be due to the pre-processing `BMI-FGSM` applies. However, it was then able to perform a successful prediction

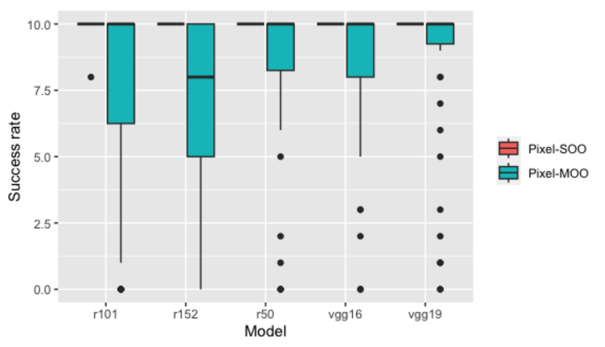

Fig. 3: Success rate of both approaches on each model

flip to 'Model T' (272). while Pixel−SOO successfully flipped it from the correct class to a 'coyote' (58). Fig. 2 depicts (1) the original image, (2) the 'perturbation mask', and (3) the resulting adversarial attacks.

We can observe that, for BMI−FGSM, the median amount of changed pixels is 4325 and for Pixel−SOO is 25, which is a remarkable difference. From Fig. 2, we can barely see any modification in the change matrix, and this is because BMI−FGSM subtly changes many pixels. Our method, however, stands out for the smallest amount of perturbations which involves making larger color differences to the pixel. However, as we can see by the matrix and the final image, the changes applied are still very subtle.

On top of having considerably fewer perturbations and a better success rate, we observe from Table I that the number of generations required by Pixel−SOO and Pixel−MOO is also much lower than the generations needed by BMI−FGSM for converging. BMI−FGSM took on average 240 generations to reach a prediction flip, while our Pixel−SOO method took only 10, once again being considerably quicker.

Results on other models. The original BMI−FGSM implementation (which we have reused) was not compatible with the other models except for the ResNet models. However, in our experiment, BMI−FGSM took a considerable amount of time to complete just a single run (often over 7 hours) and often could not generate any adversarial example within the search budget. In the following, we therefore only report the results for the two DE-based approaches proposed in this paper, namely Pixel−SOO and Pixel−MOO.

Figure 3 depicts boxplots for the success rate over the different runs of Pixel−MOO and Pixel−SOO for the five DNN models in our study. As we can observe, Pixel−SOO is successful almost 100% of the time, with some outliers only for ResNet101. Pixel−MOO still achieves a 100% success rate for more than 50% of the images.

These differences are also confirmed by Fisher's exact test, of which the results are reported in Table II. More specifically, Pixel−MOO and Pixel−SOO are statistically equivalent in terms of success rate for the large majority of the images (success rate over ten runs) and across all models. For around 20% of images, the single-objective variants statistically outperform the multi-objective variant. For ResNet101

TABLE II: Number of times one approach outperforms the other according to the Fisher's test (p-value$<$0.05) w.r.t. the Success Rate

Model	Pixel−MOO wins	Equal	Pixel−SOO wins
r50	-	44	6
r101	-	33	17
r152	-	42	8
vgg16	-	39	11
vgg19	-	43	7

TABLE III: Number of times one approach outperforms the other according to the Wilcoxon test (p-value$<$0.05) and the $\hat{A}_{12}$ statistics w.r.t. the number of changed pixels.

Model	Pixel−MOO wins			Equal	Pixel−SOO win		
	Large	Medium	Small		Small	Medium	Large
r50	28	7	-	15	-	-	-
r101	33	3	-	13	-	1	-
r152	28	3	-	19	-	-	-
vgg16	26	6	-	18	-	-	-
vgg19	29	7	-	14	-	-	-

in particular, Pixel−SOO frequently has a higher success rate compared to its multi-objective counterpart. As Pixel−MOO searches for trade-offs between prediction flip ($O1$) whilst preserving as many original pixel values as possible ($O2$), we hypothesize it may be slower to reach optima in comparison to Pixel−SOO, and may perform better when a larger search budget (i.e., more generations) would be used.

Finally, we compare the attacks generated by Pixel−MOO and Pixel−SOO w.r.t. the number of pixel perturbations injected in the seed images. Table III reports the results of the Wilcoxon rank sum test and the $\hat{A}_{12}$ statistics. The results indicate that the adversarial attacks generated by Pixel−MOO contain fewer pixel alterations than those produced by Pixel−SOO, and the results are statistically significant in more than 60% of the comparison, with an effect size being *large* in the large majority of the significant cases.

Therefore, we can draw some general conclusion: Pixel−MOO and Pixel−SOO provide two different trade-offs concerning the speed and magnitude of the image perturbation. Pixel−SOO is faster by producing attacks with less subtle changes. Instead, Pixel−MOO produced more subtle attacks but requires more time to converge.

V. Threats to Validity

Internal validity. While our image selection procedure yielded a random draw of images from 50 unique classes, the ILSVRC2012 classes semantically are not uniformly distributed (e.g. having multiple classes with sub-species of dogs). Future sampling strategies could seek to more explicitly mitigate for this.

External validity. Currently, our approach was only was tested against (the state-of-the-art) BMI−FGSM. It will be worthwhile to also test it against further attack approaches, such as the one-pixel attack [30]. Furthermore, beyond our current set of DNN models, more canonical models exist that can be studied, such as Inception-v3 [33].

Conclusion validity. In some runs, `Pixel-MOO` fails to find an adversarial example; further optimizations w.r.t. population and generation size may be needed.

VI. Conclusion and Future Work

In this paper, we have introduced two approaches based on pure differential evolution, namely `Pixel-MOO` and `Pixel-SOO`, with customized differential operators for generating adversarial example. Our empirical study with multiple DNN models for image recognition showed that: (1) both approaches outperform the state-of-the-art `BMI-FGSM` in terms of success rate and by applying fewer (yet subtle) pixel changes, and (2) `Pixel-SOO` and `Pixel-MOO` provide two different trade-offs in terms of convergence speed (`Pixel-SOO` is faster) and subtler changes (`Pixel-MOO` applies fewer pixel changes).

In our future work, it will be worthwhile to more explicitly look at the potential difficulty of images due to semantic ambiguity, which already can show in the initial classification confidence of a model [18]. Furthermore, we intend to extend our comparison to multiple deep learning models, and different search algorithms (e.g., MOEA/D [38] and AGE-MOEA [24]) or combine the strengths of `Pixel-MOO` and `Pixel-SOO` with hybrid approaches.

References

[1] Scalable parallel programming with cuda. In: 2008 IEEE Hot Chips 20 Symposium (HCS). pp. 1–2 (2008)

[2] Angira, R., Babu, B.: Non-dominated sorting differential evolution (nsde): An extension of differential evolution for multi-objective optimization. In: IICAI. pp. 1428–1443 (2005)

[3] Blank, J., Deb, K.: pymoo: Multi-objective optimization in python. IEEE Access **8**, 89497–89509 (2020)

[4] Chan, K., Cheng, B.H.: Evoattack: An evolutionary search-based adversarial attack for object detection models. In: International Symposium on Search-Based Software Engineering. pp. 83–97. Springer (2022)

[5] Chollet, F., et al.: Keras. https://keras.io (2015)

[6] Chugh, T., Sindhya, K., Hakanen, J., Miettinen, K.: A survey on handling computationally expensive multiobjective optimization problems with evolutionary algorithms. Soft Computing **23** (2019)

[7] Conover, W.J.: Practical nonparametric statistics, vol. 350. John Wiley & Sons (1998)

[8] Deb, K., Pratap, A., Agarwal, S., Meyarivan, T.: A fast and elitist multiobjective genetic algorithm: Nsga-ii. IEEE transactions on evolutionary computation **6**(2), 182–197 (2002)

[9] Fisher, R.A.: Statistical methods for research workers. In: Breakthroughs in statistics, pp. 66–70. Springer (1992)

[10] Ghamizi, S., Cordy, M., Gubri, M., Papadakis, M., Boystov, A., Le Traon, Y., Goujon, A.: Search-Based Adversarial Testing and Improvement of Constrained Credit Scoring Systems. Association for Computing Machinery, New York, NY, USA (2020)

[11] Goodfellow, I.J., Shlens, J., Szegedy, C.: Explaining and harnessing adversarial examples. In: Proceedings of the International Conference on Learning Representations (ICLR) (2015)

[12] Guo, J., Zhao, Y., Song, H., Jiang, Y.: Coverage guided differential adversarial testing of deep learning systems. IEEE Transactions on Network Science and Engineering **8**(2), 933–942 (2021)

[13] He, K., Zhang, X., Ren, S., Sun, J.: Deep residual learning for image recognition (2015). https://doi.org/10.48550/ARXIV.1512.03385

[14] Ishida, S., Ono, S.: Adjust-free adversarial example generation in speech recognition using evolutionary multi-objective optimization under black-box condition **26**(2) (2021)

[15] Khare, S., Aralikatte, R., Man, S.: Adversarial Black-Box Attacks on Automatic Speech Recognition Systems using Multi-Objective Evolutionary Optimization. In: Proceedings of INTERSPEECH (2019)

[16] Kim, J., Feldt, R., Yoo, S.: Guiding deep learning system testing using surprise adequacy. IEEE Press (2019)

[17] Krizhevsky, A.: Learning multiple layers of features from tiny images. Tech. rep. (2009)

[18] Liem, C.C.S., Panichella, A.: Oracle Issues in Machine Learning and Where To Find Them. In: Proceedings of the IEEE/ACM 42nd International Conference on Software Engineering Workshops (2020)

[19] Lin, J., Xu, L., Liu, Y., Zhang, X.: Black-box adversarial sample generation based on differential evolution (2020)

[20] Ma, L., Zhang, F., Sun, J., Xue, M., Li, B., Juefei-Xu, F., Xie, C., Li, L., Liu, Y., Zhao, J., Wang, Y.: DeepMutation: Mutation testing of deep learning systems. In: Proceedings of the 29th International Symposium on Software Reliability Engineering (ISSRE) (2018)

[21] Montgomery, J., Chen, S.: An analysis of the operation of differential evolution at high and low crossover rates. In: IEEE congress on evolutionary computation. pp. 1–8. IEEE (2010)

[22] Moosavi-Dezfooli, S.M., Fawzi, A., Frossard, P.: Deepfool: a simple and accurate method to fool deep neural networks (2015). https://doi.org/10.48550/ARXIV.1511.04599

[23] Nguyen, A., Yosinski, J., Clune, J.: Deep neural networks are easily fooled: High confidence predictions for unrecognizable images. In: Proceedings of the 2015 IEEE Conference on Computer Vision and Pattern Recognition (CVPR) (2015)

[24] Panichella, A.: An adaptive evolutionary algorithm based on non-euclidean geometry for many-objective optimization. In: Proceedings of the Genetic and Evolutionary Computation Conference. pp. 595–603 (2019)

[25] Pei, K., Cao, Y., Yang, J., Jana, S.: Deepxplore: Automated whitebox testing of deep learning systems **62**(11) (2019)

[26] Russakovsky, O., Deng, J., Su, H., Krause, J., Satheesh, S., Ma, S., Huang, Z., Karpathy, A., Khosla, A., Bernstein, M., Berg, A.C., Fei-Fei, L.: ImageNet Large Scale Visual Recognition Challenge. Int. J. Computer Vision **115**(3), 211–252 (2015)

[27] Salimans, T., Ho, J., Chen, X., Sidor, S., Sutskever, I.: Evolution strategies as a scalable alternative to reinforcement learning. arXiv preprint arXiv:1703.03864 (2017)

[28] Simonyan, K., Zisserman, A.: Very deep convolutional networks for large-scale image recognition. In: Proceedings of the 3rd International Conference on Learning Representations (ICLR) (2015)

[29] Storn, R., Price, K.: Differential evolution – a simple and efficient heuristic for global optimization over continuous spaces **11**(4) (1997)

[30] Su, J., Vargas, D.V., Sakurai, K.: One pixel attack for fooling deep neural networks. IEEE Transactions on Evolutionary Computation **23**(5), 828–841 (oct 2019). https://doi.org/10.1109/tevc.2019.2890858

[31] Sun, W., Jin, J., Lin, W.: Minimum Noticeable Difference based Adversarial Privacy Preserving Image Generation (2022), https://arxiv.org/abs/2206.08638

[32] Suzuki, T., Takeshita, S., Ono, S.: Adversarial Example Generation using Evolutionary Multi-objective Optimization. In: 2019 IEEE Congress on Evolutionary Computation (CEC). pp. 2136–2144 (2019)

[33] Szegedy, C., Vanhoucke, V., Ioffe, S., Shlens, J., Wojna, Z.: Rethinking the inception architecture for computer vision. In: Proceedings of the IEEE conference on computer vision and pattern recognition. pp. 2818–2826 (2016)

[34] Szegedy, C., Zaremba, W., Sutskever, I., Bruna, J., Erhan, D., Goodfellow, I., Fergus, R.: Intriguing properties of neural networks. In: Proceedings of the International Conference on Learning Representations (ICLR) (2014)

[35] Tian, Y., Pei, K., Jana, S., Ray, B.: Deeptest: Automated testing of deep-neural-network-driven autonomous cars. Association for Computing Machinery, New York, NY, USA (2018)

[36] Vargha, A., Delaney, H.D.: A critique and improvement of the cl common language effect size statistics of mcgraw and wong. Journal of Educational and Behavioral Statistics **25**(2), 101–132 (2000)

[37] Zhang, P., Ren, B., Dong, H., Dai, Q.: Cagfuzz: Coverage-guided adversarial generative fuzzing testing for image-based deep learning systems. IEEE Transactions on Software Engineering pp. 1–1 (2021)

[38] Zhang, Q., Li, H.: Moea/d: A multiobjective evolutionary algorithm based on decomposition. IEEE Transactions on evolutionary computation **11**(6), 712–731 (2007)

[39] Zhou, Tan, Z.K.H.H.: An evolutionary-based black-box attack to deep neural network classifiers (2021), https://doi.org/10.1007/s11036-019-01499-x